The Astronomical Journal, 142:87 (7pp), 2011 September doi:10.1088/0004-6256/142/3/87


# THE ORBIT OF THE CEPHEID V350 Sgr REVISITED

Nancy Remage Evans[1], Leonid Berdnikov[2,3], Natalia Gorynya[2,4], Alexey Rastorguev[2], and Joel Eaton[5]
[1] Smithsonian Astrophysical Observatory, MS 4, 60 Garden Street, Cambridge, MA 02138, USA; nevans@cfa.harvard.edu
[2] Sternberg Astronomical Institute of the Moscow State University, 13 Universitetskii Prospect, Moscow 119992, Russia
[3] Isaac Newton Institute of Chile, Moscow Branch, 13 Universitetskij Prospect, Moscow 119992, Russia
[4] Institute of Astronomy of Russian Academy of Sciences, 48 Pyatnitskaya Str., Moscow, Russia
[5] 7050 Bakerville Road, Waverly, TN 37185, USA; nevans@cfa.harvard.edu
*Received 2011 June 15; accepted 2011 July 14; published 2011 August 16*

## ABSTRACT

"The Cepheid Mass Problem" is one of the fundamental tests of the understanding of stellar evolution. One of the foundations of measured masses for Cepheids for this question is binary orbits. V350 Sgr is a classical Cepheid in a binary system. New radial velocity data for the system have been obtained over the last several years, and are used to update the orbit. The secondary in the system has previously had its orbital velocity amplitude measured in the ultraviolet with the *Hubble Space Telescope*. This amplitude has been combined with the new orbit and the adopted mass of the secondary resulting in a Cepheid mass of $5.0 \pm 0.8\ M_{\odot}$.

*Key words:* binaries: spectroscopic – stars: massive – stars: variables: Cepheids

*Online-only material:* color figures, machine-readable and VO tables

## 1. INTRODUCTION

For the last half century since computing power allowed the comparison of evolutionary tracks with hydrodynamic pulsation calculations for classical Cepheids, there has been a mismatch between the masses computed by these two approaches. Improvements in envelop opacities and main-sequence convective core overshoot have reduced the discrepancy. Recent discussions of the remaining problem are found in Caputo et al. (2005), Bono et al. (2006), and Keller (2008). Particular interest in this topic was generated recently by the mass determined from an eclipsing binary system containing a Cepheid in the Large Magellanic Cloud (LMC; Pietrzynski et al. 2010; Cassisi & Salaris 2011). The two areas most likely to provide insight into this question are the treatment of convective overshoot (the size of the He-burning core) and possible mass loss (Neilson et al. 2011; Marengo et al. 2010).

On the observational side, masses have been measured for a few galactic Cepheids (summarized in the Discussion section below). V350 Sgr is one of the few classical Cepheids which is a member of a binary system for which an orbit has been determined. Furthermore, the orbital velocity amplitude is large and a mass can be determined for the Cepheid from an orbital velocity amplitude of the hot companion measured in the ultraviolet. Evans et al. (1997) have done this for V350 Sgr, based on an orbit for the Cepheid (Evans & Sugars 1997). Since that time, considerable additional radial velocity data have been obtained, making it useful to provide an updated orbit. Since the orbital period is very close to four years, it is difficult to get even coverage of the orbit. The new data provide better coverage of orbital velocity minimum, resulting in a more accurate orbital velocity amplitude. In the sections below, the new data are presented, the pulsation period is discussed, the pulsation velocity curve has been revisited, and the observed velocities (corrected for the pulsation velocity) are used to derive a new orbit.

## 2. VELOCITIES

We have collected two extensive new sets of radial velocities at Tennessee State University and Moscow University and added to them some other recent data from the literature. These new data provide an improved orbital solution, particularly the amplitude, which is the crucial quantity for mass determination.

Eaton obtained high-dispersion spectra of V350 Sgr covering five years (2005 February to 2009 October) with the Tennessee State University 2 m Automatic Spectroscopic Telescope (AST). The AST is an echelle system, covering the wavelength range 5000–7100 Å, with a resolution of approximately 30,000. Velocities were measured from these spectra with a cross-correlation technique (see Bruntt et al. 2008 and Eaton & Williamson (2007, and references therein for details). We have added a correction of +0.35 km $s^{-1}$ to the measured velocities (J. Eaton 2010, private communication) to place them on the IAU velocity system. These velocities are listed as Source 7 in Table 1, which we give in its entirety in the online version of this journal in the same format as the first few lines presented here. The first two columns are Heliocentric Julian Date and the observed velocity; the data source, identified in Table 2, is listed in the final column. The phases and results of the velocity solution in the other four columns are discussed in the following sections.

New data have also been obtained by the Moscow University radial velocity program. The measurements are made with a CORAVEL-type spectrometer (Tokovinin 1987) from 1987 to 2010. Spectral resolution is approximately 20,000 in the wavelength interval 3700–6500 Å. The template spectrum is from Arcturus. Data have been collected using many telescopes (0.6 m Zeiss telescopes in the Crimean (Ukraine) and Maidanak (Uzbekistan) observatories, 1.0 m Zeiss telescopes in Maidanak (Uzbekistan) and Simeiz (Ukraine) observatories). Data though 1994 have been discussed by Evans & Sugars (1997). The new data comprise 61 velocities obtained between 1995 June and 2008 June. Publication of the new data is in preparation, and will ultimately include 168 northern Cepheids. The full list of observations for V350 Sgr is included in the online version of this journal.

All the velocity data sets used in our new analysis are listed in Table 2 with individual velocities given in Table 1. In addition to the extensive AST and more recent Moscow University velocities that are mentioned above, we have used previously published radial velocity data from several other sources (Table 2). Evans & Sugars (1997) discussed the data

**Table 1**
Radial Velocities and Orbit

| HJD −2,400,000 | $V_{Tot}$[a] (km s$^{-1}$) | $\phi_{Orb}$ | $\phi_{Pul}$ | $V_{Orb}$ (km s$^{-1}$) | $O-C$ (km s$^{-1}$) | Source |
|---|---|---|---|---|---|---|
| 47370.3540 | 8.58 | 0.857 | 0.536 | 1.43 | 1.11 | 1. |
| 48422.4430 | 21.09 | 0.571 | 0.657 | 8.02 | 1.04 | 1. |
| 48423.4660 | 22.68 | 0.572 | 0.855 | 8.00 | 0.87 | 1. |
| 48424.4660 | −9.02 | 0.573 | 0.049 | 7.98 | −0.15 | 1. |
| 48426.4540 | 9.39 | 0.574 | 0.435 | 7.93 | −0.23 | 1. |
| 48428.4680 | 27.99 | 0.575 | 0.826 | 7.89 | 2.28 | 1. |
| 48433.4200 | 26.96 | 0.579 | 0.787 | 7.78 | 0.55 | 1. |
| 48437.3890 | 16.41 | 0.582 | 0.557 | 7.70 | 1.59 | 1. |
| 48439.4450 | −3.20 | 0.583 | 0.955 | 7.66 | 0.14 | 1. |

**Note.**
[a] Radial velocities are listed including two decimal places for the purpose of the solution; however, they are only accurate to a single decimal place at best.

(This table is available in its entirety in machine-readable and Virtual Observatory (VO) forms in the online journal. A portion is shown here for guidance regarding its form and content.)

**Table 2**
Velocity Sources for V350 Sgr

| Source | No. Vels | rms (km s$^{-1}$) | Ref. |
|---|---|---|---|
| 1 | 137 | 1.145 | Gorynya et al. (1992, 1996, 1998) |
| 2 | 16 | 0.540 | Petterson et al. (2004) |
| 3 | 40 | 1.209 | Evans & Sugars (1997) |
| 5 | 19 | 1.344 | Gieren (1981a) |
| 6 | 20 | 2.034 | Lloyd Evans (1980) |
| 7 | 104 | 0.528 | Eaton, Table 1 |

available up to that time. Since then, Petterson et al. (2004) have obtained a number of additional velocities at Mount John University Observatory. For completeness sake, we mention two other velocity data sets of V350 Sgr that have not been used. The very early velocities of Joy (1937) have been excluded because they are from comparatively low dispersion, 75 Å mm$^{-1}$ at H$\gamma$, spectra. Also not used are the velocities of Barnes et al. (1988) that have a velocity scatter that is considerably larger than the other data (originally Source 4 in Table 2).

## 3. PULSATION PERIOD

Before the observed velocities can be used to determine the orbit, they must be corrected for the pulsation velocities. The first step is to obtain an accurate pulsation period, particularly when the velocity data extend over a long period, as they do for V350 Sgr. To study period changes, we applied the standard technique of the analysis of $O-C$ diagrams. We calculated the $O-C$ residuals by the Hertzsprung (1919) method, using a computer version which was previously developed and described by one of us (Berdnikov 1992). In the case of photoelectric observations, we reduced the measurements both in the yellow (the $V$ band of Johnson's photometric system or measurements in yellow bands of various systems transformed to $V$) and in the blue (the $B$ band of Johnson's broadband system or measurements in blue bands of various systems transformed to $B$). The photographic and visual observations were reduced in the same manner as $B$ and $V$ photoelectric measurements. The results of reductions using Hertzsprung's method are summarized in Table 3. The first and second columns give the times of light maximum with their estimated uncertainties, the third column indicates the type of observations: PG and VIS for photographic

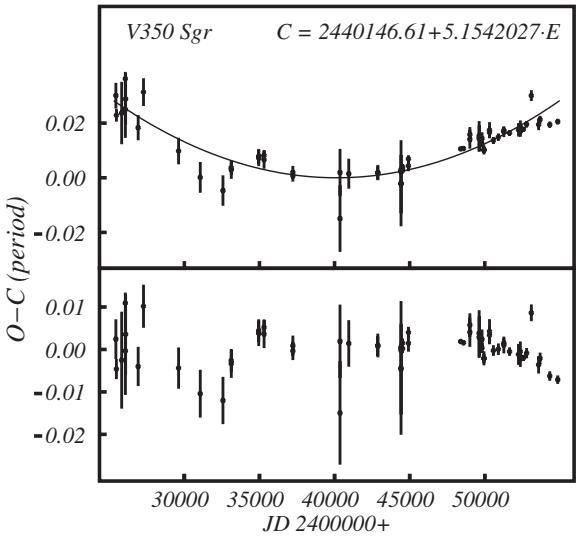


**Figure 1.** $O-C$ diagrams for times of maximum light (in period phase). Top: times of maximum (dots) with the changing period solution (solid line). Bottom: residuals from the changing period solution.

and visual observations, and $B$ and $V$ for photoelectric observations in the $B$ and $V$ filters. The fourth and fifth columns contain the epoch number $E$ and the residual $O-C$; the sixth and seventh columns present the number of observations reduced and references for the sources of data. It should be noted that our results refer to particular standard curves. Therefore, we present them in Table 4 to make them available to other authors either for use in their future studies or for finding relationships with our data when different standard curves are used. Table 4 contains $B$ and $V$ magnitudes of the Cepheids for phases from 0 to 0.995, sampled at intervals of 0.005. Based on the best photoelectric observations, we found the maxima in the $B$ band to occur earlier than those in the $V$ band by 0.0055 days. We applied this correction in constructing the $O-C$ diagram (Figure 1) and determining elements, which, thus, refer to the $V$ band.

The linear part of these elements was used to calculate the $O-C$ residuals in the fifth column of Table 3 and to construct the upper part of Figure 1 where $O-C$ residuals are plotted by circles with vertical bars showing the uncertainty limits. For convenience, we express the $O-C$ residuals in fractions of the period. The parabolic fit to the $O-C$ diagram in Figure 1 indicates a changing period. Deviations from the fit are shown in the bottom panel. This fit has been used to determine the pulsation phases of the velocities:

$$\begin{aligned}\text{Max JD} = {} & 2{,}440{,}146.6156 + 5.15420271E \\ & + 0.1751265 \times 10^{-07}E^2 \\ & \pm 0.0055 \pm 0.00000176 \pm 0.01227409 \times 10^{-07}.\end{aligned}$$

This corresponds to a period change of $0.35 \times 10^{-07}$ days cycle$^{-1}$ or 0.21 s yr$^{-1}$ with an uncertainty of about 7%.

For the data in Table 1, we have used the period $5^{d}.15425024$. The maximum difference between this and the full quadratic version above is only 0.006 in pulsation phase, which is insignificant.

**Table 3**
Times of Maximum Light of V350 Sgr

| Max JD Hel | Uncertainty | Filter | $E$ | $O-C$ | $N$ | Reference |
|---|---|---|---|---|---|---|
| 2425441.8244 | 0.0241 | PG | −2853 | 0.1491 | 20 | Albitzky (1930) |
| 2425477.8668 | 0.0122 | PG | −2846 | 0.1121 | 237 | Voute (1932) |
| 2425828.3626 | 0.0589 | VIS | −2778 | 0.1221 | 44 | Parenago (1930) |
| 2426070.6690 | 0.0128 | PG | −2731 | 0.1810 | 237 | Voute (1932) |
| 2426075.7710 | 0.0535 | VIS | −2730 | 0.1288 | 81 | Parenago (1938) |
| 2426091.2534 | 0.0484 | VIS | −2727 | 0.1486 | 72 | Kukarkin (1940) |
| 2426926.1802 | 0.0238 | VIS | −2565 | 0.0945 | 102 | Florya & Kukarkina (1953) |
| 2427281.8872 | 0.0262 | VIS | −2496 | 0.1616 | 95 | Florya & Kukarkina (1953) |
| 2429616.6240 | 0.0251 | PG | −2043 | 0.0446 | 138 | Filin (1950) |
| 2431059.7511 | 0.0290 | PG | −1763 | −0.0052 | 103 | Filin (1950) |
| 2432569.9076 | 0.0287 | PG | −1470 | −0.0300 | 106 | Filin (1950) |
| 2433121.4504 | 0.0133 | *B* | −1363 | 0.0131 | 13 | Eggen (1951) |
| 2433126.6068 | 0.0173 | *V* | −1362 | 0.0153 | 12 | Eggen (1951) |
| 2434951.2141 | 0.0137 | *B* | −1008 | 0.0348 | 10 | Walraven et al. (1958) |
| 2434951.2165 | 0.0153 | *V* | −1008 | 0.0372 | 10 | Walraven et al. (1958) |
| 2435306.8533 | 0.0170 | *V* | −939 | 0.0340 | 5 | Irwin (1961) |
| 2435306.8556 | 0.0097 | *B* | −939 | 0.0363 | 5 | Irwin (1961) |
| 2437224.1806 | 0.0111 | *B* | −567 | −0.0021 | 14 | Mitchell et al. (1964) |
| 2437224.1928 | 0.0123 | *V* | −567 | 0.0101 | 14 | Mitchell et al. (1964) |
| 2440363.0150 | 0.0628 | *V* | 42 | −0.0771 | 7 | Stobie (1970) |
| 2440363.0962 | 0.0445 | *B* | 42 | 0.0041 | 7 | Stobie (1970) |
| 2440945.5247 | 0.0283 | *V* | 155 | 0.0077 | 34 | Feltz & McNamara (1980) |
| 2442878.3461 | 0.0119 | *B* | 530 | 0.0031 | 6 | Dean (1977) |
| 2442878.3528 | 0.0144 | *V* | 530 | 0.0098 | 6 | Dean (1977) |
| 2444414.3009 | 0.0017 | *B* | 828 | 0.0055 | 34 | Gieren (1981b) |
| 2444414.3102 | 0.0018 | *V* | 828 | 0.0148 | 34 | Gieren (1981b) |
| 2444424.5861 | 0.0552 | *B* | 830 | −0.0177 | 4 | Caldwell et al. (2001) |
| 2444424.5935 | 0.0812 | *V* | 830 | −0.0103 | 4 | Caldwell et al. (2001) |
| 2444527.6957 | 0.0054 | *B* | 850 | 0.0078 | 23 | Moffett & Barnes (1984) |
| 2444527.7083 | 0.0056 | *V* | 850 | 0.0204 | 23 | Moffett & Barnes (1984) |
| 2444919.4299 | 0.0103 | *V* | 926 | 0.0226 | 14 | Eggen (1985) |
| 2444919.4371 | 0.0068 | *B* | 926 | 0.0298 | 14 | Eggen (1985) |
| 2448393.3944 | 0.0027 | *V* | 1600 | 0.0545 | 45 | ESA (1997) |
| 2448584.1006 | 0.0031 | *V* | 1637 | 0.0552 | 55 | ESA (1997) |
| 2449006.7627 | 0.0178 | *V* | 1719 | 0.0726 | 18 | Arellano Ferro et al. (1998) |
| 2449006.7656 | 0.0142 | *B* | 1719 | 0.0755 | 18 | Arellano Ferro et al. (1998) |
| 2449625.2673 | 0.0281 | *B* | 1839 | 0.0729 | 10 | Berdnikov & Vozyakova (1995) |
| 2449625.2685 | 0.0252 | *V* | 1839 | 0.0741 | 10 | Berdnikov & Vozyakova (1995) |
| 2449815.9575 | 0.0063 | *B* | 1876 | 0.0576 | 16 | Berdnikov & Turner (1995) |
| 2449815.9740 | 0.0118 | *V* | 1876 | 0.0741 | 16 | Berdnikov & Turner (1995) |
| 2449944.8015 | 0.0055 | *B* | 1901 | 0.0465 | 18 | Berdnikov et al. (1997) |
| 2449944.8074 | 0.0085 | *V* | 1901 | 0.0524 | 21 | Berdnikov et al. (1997) |
| 2450315.9372 | 0.0111 | *B* | 1973 | 0.0797 | 19 | Berdnikov et al. (1998) |
| 2450315.9477 | 0.0148 | *V* | 1973 | 0.0902 | 19 | Berdnikov et al. (1998) |
| 2450573.6380 | 0.0065 | *V* | 2023 | 0.0703 | 28 | Berdnikov & Turner (1998) |
| 2450903.5132 | 0.0070 | *V* | 2087 | 0.0765 | 28 | Berdnikov & Turner (2000) |
| 2451269.4685 | 0.0055 | *B* | 2158 | 0.0835 | 24 | Berdnikov & Turner (2001) |
| 2451269.4720 | 0.0102 | *V* | 2158 | 0.0870 | 24 | Berdnikov & Turner (2001) |
| 2451650.8807 | 0.0052 | *V* | 2232 | 0.0847 | 21 | Berdnikov & Caldwell (2001) |
| 2452243.6198 | 0.0127 | *V* | 2347 | 0.0905 | 64 | Pojmanski (2002) |
| 2452367.3116 | 0.0100 | *B* | 2371 | 0.0814 | 27 | Berdnikov & Turner (2004) |
| 2452367.3261 | 0.0123 | *V* | 2371 | 0.0959 | 27 | Berdnikov & Turner (2004) |
| 2452573.4898 | 0.0038 | *V* | 2411 | 0.0915 | 135 | Pojmanski (2002) |
| 2452784.8215 | 0.0062 | *V* | 2452 | 0.1008 | 86 | Pojmanski (2002) |
| 2453099.2821 | 0.0102 | *V* | 2513 | 0.1551 | 15 | Berdnikov & Turner (2006) |
| 2453583.7224 | 0.0106 | *V* | 2607 | 0.1004 | 91 | Pojmanski (2002) |
| 2453681.6618 | 0.0069 | *V* | 2626 | 0.1099 | 86 | Pojmanski (2002) |
| 2454325.9275 | 0.0058 | *V* | 2751 | 0.1003 | 100 | Pojmanski (2002) |
| 2454856.8161 | 0.0052 | *V* | 2854 | 0.1059 | 100 | Pojmanski (2002) |

## 4. THE CONTRIBUTION OF PULSATION TO THE RADIAL VELOCITIES

The pulsation of the Cepheid contributes to the measured radial velocity. The actual motion of the photosphere is, of course, the velocity projected over the surface elements, including the effect of limb darkening. In this section we discuss the correction for this motion (which we refer to as "the pulsation velocity" below) to obtain the orbital velocity. This correction can be done in a number of ways, including digitizing the pulsation curve

**Table 4**
Standard Curves of the Cepheid V350 Sgr in Filters *B* and *V*

| Phase | *B* | *V* | Phase | *B* | *V* | Phase | *B* | *V* | Phase | *B* | *V* |
|---|---|---|---|---|---|---|---|---|---|---|---|
| 0.000 | 7.812 | 7.086 | 0.250 | 8.311 | 7.398 | 0.500 | 8.694 | 7.646 | 0.750 | 8.848 | 7.794 |
| 0.005 | 7.813 | 7.086 | 0.255 | 8.322 | 7.404 | 0.505 | 8.699 | 7.650 | 0.755 | 8.842 | 7.790 |
| 0.010 | 7.816 | 7.088 | 0.260 | 8.333 | 7.410 | 0.510 | 8.704 | 7.655 | 0.760 | 8.834 | 7.785 |
| 0.015 | 7.820 | 7.091 | 0.265 | 8.343 | 7.415 | 0.515 | 8.708 | 7.659 | 0.765 | 8.826 | 7.780 |
| 0.020 | 7.826 | 7.095 | 0.270 | 8.354 | 7.421 | 0.520 | 8.713 | 7.663 | 0.770 | 8.816 | 7.774 |
| 0.025 | 7.833 | 7.099 | 0.275 | 8.365 | 7.427 | 0.525 | 8.717 | 7.668 | 0.775 | 8.805 | 7.768 |
| 0.030 | 7.841 | 7.104 | 0.280 | 8.375 | 7.432 | 0.530 | 8.722 | 7.672 | 0.780 | 8.793 | 7.760 |
| 0.035 | 7.850 | 7.110 | 0.285 | 8.385 | 7.438 | 0.535 | 8.726 | 7.677 | 0.785 | 8.780 | 7.752 |
| 0.040 | 7.860 | 7.117 | 0.290 | 8.396 | 7.444 | 0.540 | 8.730 | 7.681 | 0.790 | 8.766 | 7.743 |
| 0.045 | 7.871 | 7.123 | 0.295 | 8.405 | 7.450 | 0.545 | 8.734 | 7.685 | 0.795 | 8.750 | 7.734 |
| 0.050 | 7.883 | 7.130 | 0.300 | 8.415 | 7.455 | 0.550 | 8.739 | 7.690 | 0.800 | 8.733 | 7.723 |
| 0.055 | 7.894 | 7.137 | 0.305 | 8.424 | 7.461 | 0.555 | 8.743 | 7.694 | 0.805 | 8.715 | 7.712 |
| 0.060 | 7.907 | 7.145 | 0.310 | 8.433 | 7.467 | 0.560 | 8.747 | 7.698 | 0.810 | 8.696 | 7.700 |
| 0.065 | 7.919 | 7.152 | 0.315 | 8.442 | 7.473 | 0.565 | 8.752 | 7.702 | 0.815 | 8.675 | 7.687 |
| 0.070 | 7.932 | 7.160 | 0.320 | 8.450 | 7.479 | 0.570 | 8.757 | 7.707 | 0.820 | 8.654 | 7.673 |
| 0.075 | 7.945 | 7.167 | 0.325 | 8.458 | 7.485 | 0.575 | 8.761 | 7.711 | 0.825 | 8.631 | 7.658 |
| 0.080 | 7.957 | 7.174 | 0.330 | 8.465 | 7.490 | 0.580 | 8.766 | 7.715 | 0.830 | 8.607 | 7.643 |
| 0.085 | 7.970 | 7.182 | 0.335 | 8.473 | 7.496 | 0.585 | 8.771 | 7.720 | 0.835 | 8.581 | 7.626 |
| 0.090 | 7.982 | 7.189 | 0.340 | 8.479 | 7.502 | 0.590 | 8.776 | 7.724 | 0.840 | 8.555 | 7.609 |
| 0.095 | 7.995 | 7.196 | 0.345 | 8.486 | 7.507 | 0.595 | 8.782 | 7.728 | 0.845 | 8.528 | 7.591 |
| 0.100 | 8.007 | 7.203 | 0.350 | 8.492 | 7.513 | 0.600 | 8.787 | 7.733 | 0.850 | 8.499 | 7.572 |
| 0.105 | 8.019 | 7.210 | 0.355 | 8.499 | 7.518 | 0.605 | 8.792 | 7.737 | 0.855 | 8.470 | 7.552 |
| 0.110 | 8.030 | 7.216 | 0.360 | 8.505 | 7.524 | 0.610 | 8.798 | 7.741 | 0.860 | 8.440 | 7.532 |
| 0.115 | 8.042 | 7.223 | 0.365 | 8.511 | 7.529 | 0.615 | 8.803 | 7.745 | 0.865 | 8.410 | 7.511 |
| 0.120 | 8.053 | 7.230 | 0.370 | 8.517 | 7.534 | 0.620 | 8.808 | 7.750 | 0.870 | 8.379 | 7.489 |
| 0.125 | 8.064 | 7.236 | 0.375 | 8.522 | 7.539 | 0.625 | 8.814 | 7.754 | 0.875 | 8.347 | 7.467 |
| 0.130 | 8.074 | 7.243 | 0.380 | 8.528 | 7.544 | 0.630 | 8.819 | 7.758 | 0.880 | 8.315 | 7.445 |
| 0.135 | 8.085 | 7.250 | 0.385 | 8.534 | 7.549 | 0.635 | 8.824 | 7.762 | 0.885 | 8.283 | 7.422 |
| 0.140 | 8.095 | 7.256 | 0.390 | 8.541 | 7.553 | 0.640 | 8.829 | 7.766 | 0.890 | 8.250 | 7.399 |
| 0.145 | 8.105 | 7.263 | 0.395 | 8.547 | 7.558 | 0.645 | 8.834 | 7.770 | 0.895 | 8.218 | 7.376 |
| 0.150 | 8.115 | 7.270 | 0.400 | 8.553 | 7.562 | 0.650 | 8.838 | 7.774 | 0.900 | 8.186 | 7.353 |
| 0.155 | 8.125 | 7.276 | 0.405 | 8.560 | 7.566 | 0.655 | 8.843 | 7.778 | 0.905 | 8.154 | 7.330 |
| 0.160 | 8.134 | 7.283 | 0.410 | 8.567 | 7.571 | 0.660 | 8.847 | 7.782 | 0.910 | 8.123 | 7.308 |
| 0.165 | 8.144 | 7.290 | 0.415 | 8.574 | 7.575 | 0.665 | 8.851 | 7.785 | 0.915 | 8.092 | 7.286 |
| 0.170 | 8.153 | 7.297 | 0.420 | 8.581 | 7.579 | 0.670 | 8.854 | 7.788 | 0.920 | 8.063 | 7.265 |
| 0.175 | 8.163 | 7.304 | 0.425 | 8.589 | 7.583 | 0.675 | 8.858 | 7.791 | 0.925 | 8.034 | 7.244 |
| 0.180 | 8.172 | 7.310 | 0.430 | 8.596 | 7.587 | 0.680 | 8.861 | 7.794 | 0.930 | 8.007 | 7.224 |
| 0.185 | 8.181 | 7.317 | 0.435 | 8.604 | 7.591 | 0.685 | 8.863 | 7.797 | 0.935 | 7.981 | 7.206 |
| 0.190 | 8.191 | 7.324 | 0.440 | 8.612 | 7.595 | 0.690 | 8.865 | 7.799 | 0.940 | 7.956 | 7.188 |
| 0.195 | 8.200 | 7.330 | 0.445 | 8.620 | 7.599 | 0.695 | 8.867 | 7.801 | 0.945 | 7.934 | 7.172 |
| 0.200 | 8.210 | 7.337 | 0.450 | 8.627 | 7.603 | 0.700 | 8.869 | 7.803 | 0.950 | 7.913 | 7.156 |
| 0.205 | 8.219 | 7.344 | 0.455 | 8.635 | 7.607 | 0.705 | 8.869 | 7.804 | 0.955 | 7.893 | 7.143 |
| 0.210 | 8.229 | 7.350 | 0.460 | 8.642 | 7.611 | 0.710 | 8.870 | 7.805 | 0.960 | 7.876 | 7.130 |
| 0.215 | 8.239 | 7.356 | 0.465 | 8.650 | 7.616 | 0.715 | 8.870 | 7.805 | 0.965 | 7.861 | 7.120 |
| 0.220 | 8.249 | 7.363 | 0.470 | 8.657 | 7.620 | 0.720 | 8.869 | 7.805 | 0.970 | 7.848 | 7.110 |
| 0.225 | 8.259 | 7.369 | 0.475 | 8.664 | 7.624 | 0.725 | 8.867 | 7.804 | 0.975 | 7.837 | 7.103 |
| 0.230 | 8.269 | 7.375 | 0.480 | 8.670 | 7.628 | 0.730 | 8.865 | 7.803 | 0.980 | 7.828 | 7.096 |
| 0.235 | 8.280 | 7.381 | 0.485 | 8.676 | 7.633 | 0.735 | 8.862 | 7.802 | 0.985 | 7.821 | 7.092 |
| 0.240 | 8.290 | 7.387 | 0.490 | 8.682 | 7.637 | 0.740 | 8.859 | 7.800 | 0.990 | 7.816 | 7.088 |
| 0.245 | 8.301 | 7.393 | 0.495 | 8.688 | 7.641 | 0.745 | 8.854 | 7.797 | 0.995 | 7.813 | 7.086 |

(Evans & Sugars 1997). However, with the very precise velocities in Table 1, and the well covered pulsation curve, a high order Fourier fit provides a very accurate representation of the pulsation curve, accurate enough that it does not add to the errors of the derived orbital motion. Figure 2 shows the pulsation curve fit with a five-term Fourier series (see the next section) of the form

$$\sum_{i=0}^{5}(a_i \sin(2\pi i\phi) + b_i \cos(2\pi i\phi)).$$

Table 5 lists the Fourier coefficients.

## 5. ORBIT

The solution for the orbit and the Fourier representation of the pulsation curve are performed simultaneously. The five orbital elements and 2N Fourier coefficients of the pulsation curve's decomposition are calculated with standard optimization algorithms from Matlab toolboxes, using $\chi^2$ statistics for minimization. The program searches for nonlinear unknowns, and fixes their values in each iteration, then finds linear coefficients by simple linear matrix division, which greatly saves processor time. With this approach, the orbit and the pulsation curve are determined without any preliminary assumptions about the

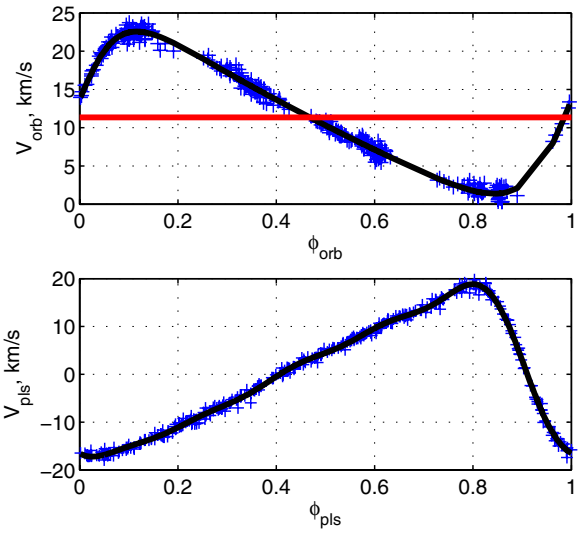


**Figure 2.** Orbit and pulsation curve for the complete data set (+'s, blue in the online version), compared orbital and pulsation solutions (solid line, black in the online version). The orbital systemic velocity is red in the online version.

(A color version of this figure is available in the online journal.)

**Table 5**
Fourier Coefficients for the Pulsation Contribution

| $i$ | $a_i$ | $b_i$ |
|---|---|---|
| 1 | −12.7885 | −7.6158 |
| 2 | −2.7022 | −5.0303 |
| 3 | 0.5087 | −2.9540 |
| 4 | 0.9778 | −1.0002 |
| 5 | 0.7306 | 0.0683 |

shape of the pulsation curve. Figure 2 illustrates that this provides a good representation of the pulsation since there is a large number of accurate data points.

The orbit in the present study is based on 40 years of modern data (10 orbital cycles), an extension of the 25 years (6 orbital cycles) available to Evans and Sugars. Table 1 lists the observations used in the solution. Columns 1 through 6 in Table 1 are the Heliocentric Julian Date, the observed velocity, the orbital phase, the pulsation phase, the computed orbital velocity, and the $O-C$ residuals. The source of the data is listed in Column 7. Figure 2 shows the orbital velocities and the velocity computed from the orbit for each point. Since the AST is a relatively new instrument, we include Figure 3 which shows the orbital curve and the pulsation curve from that data (compared with the solutions for both from the entire data set). The residuals from the final orbit for all data are presented in Figure 4 as a function of orbital phase, and as a function of pulsation phase. Although the Joy data were not used in the solution, because they are by far the earliest data, they provide a good check, particularly on the orbital period. We have examined the residuals they would have from the solution from this study, and they are reasonable for the dispersion of the spectra, and quite comparable to the residuals from the Evans and Sugars solution.

## 6. DISCUSSION/SUMMARY

The new orbital parameters are listed in Table 6. The data set for this new orbit is considerably expanded since previous solutions, and in particular, the orbital minimum velocity, are now represented by data with much higher weight, resulting

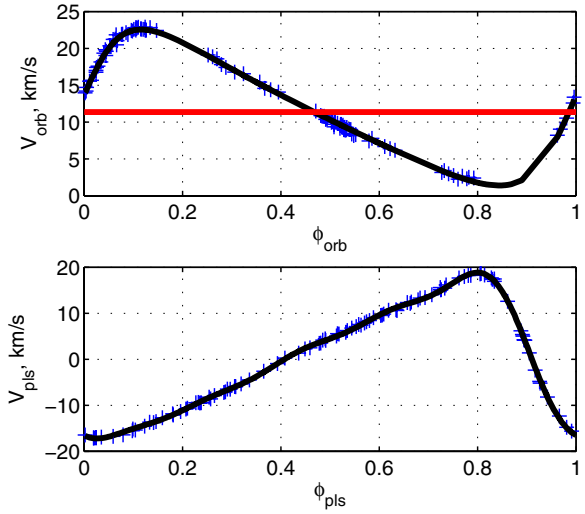


**Figure 3.** Orbit and pulsation curve for the AST data (+'s, blue in the online version), compared with the values from the solution for the complete data set (solid line, black in the online version).

(A color version of this figure is available in the online journal.)

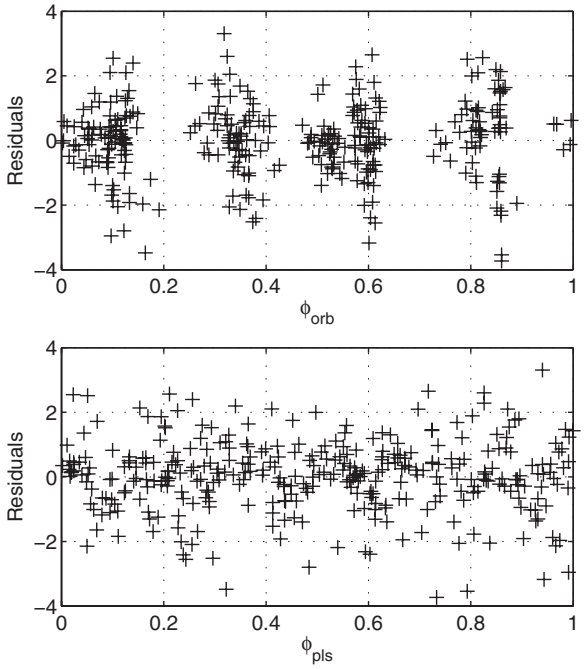


**Figure 4.** Residuals from the solution plotted as a function of orbital phase and pulsation phase.

in a more accurate orbital velocity amplitude. (Note that small differences in the systemic $\gamma$ velocity in Table 6 are expected since it depends on how the pulsation velocity was modeled.)

A mass for the Cepheid was obtained by Evans et al. (1997) by combining the orbital velocity amplitude for the Cepheid (Table 6) with two velocities for the hot companion from the *Hubble Space Telescope* (*HST*) Goddard High Resolution Spectrograph (GHRS). The two GHRS observations were made on JD −2,400,000 49474.8 and 49983.9. The velocity difference at these two orbital phases from the new orbit (Table 4) is 11.6 km s$^{-1}$. Combined with the hot star velocity difference (−23.1 km s$^{-1}$) and the mass of the hot star 2.5 $M_\odot$ (from Evans et al.), the mass of the Cepheid is now found to be 5.0 ± 0.8 $M_\odot$. The uncertainty remains essentially the same as the

**Table 6**
Orbital Elements of V350 Sgr

| Element | Evans & Sugars | Gorynya | Petterson et al. | This Study |
|---|---|---|---|---|
| $\gamma$ (km s$^{-1}$) | 11.6 ± 0.2 | 11.2 | 12.0 ± 0.2 | 11.36 ± 0.07 |
| K (km s$^{-1}$) | 10.6 ± 0.3 | 10.3 | 10.2 ± 0.04 | 10.59 ± 0.10 |
| e | 0.41 ± 0.03 | 0.31 | 0.45 ± 0.01 | 0.369 ± 0.011 |
| $\omega$ (rad) | 4.83 ± 0.05 | 5.10 | 4.82 ± 0.02 | 4.87 ± 0.03 |
| (deg) | 277. | 292. | 276. | 279. |
| $T$ (JD −2,400,000) | 40203 ± 25 | 49103 | 47604 ± 1 | 50526.63 ± 6.60 |
| $P$ (days) | 1477.0 ± 3.6 | 1467 | 1464.9 ± 0.04 | 1472.91 ± 1.33 |
| s.d. per obs. (km s$^{-1}$) | 1.16 | | | 1.161 |
| Mass function ($M_\odot$) | 0.139 ± 0.012 | 0.142 | 0.116 | 0.146 ± 0.005 |
| $a \sin i$ ($10^6$ km) | 196 ± 6 | 198 | 183.5 | 199 ± 2. |
| $a \sin i$ (AU) | 1.31 ± 0.04 | 1.32 | 1.22 | 1.33 ± 0.014 |

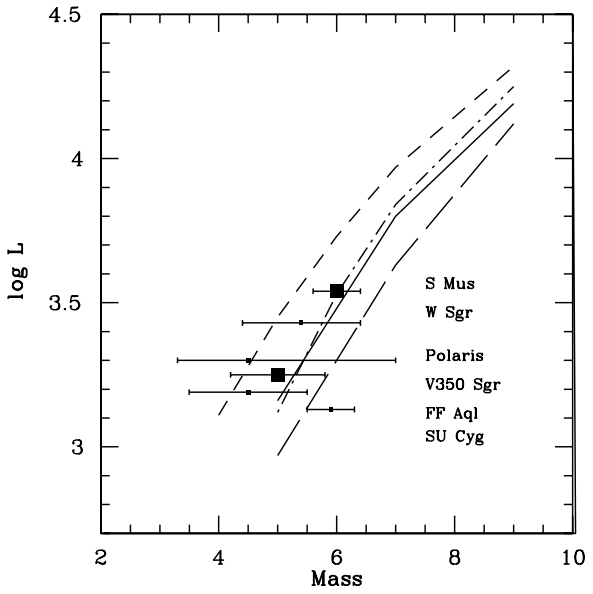


**Figure 5.** Measured masses of Cepheids. Large symbols are used for masses determined from *HST* velocities of the hot companions (see the text for discussion). Evolutionary predictions from blue loop tips are shown from left to right at the top of the figure: Padua/Bertelli et al.: full overshoot; Padua/Bertelli at al.: moderate overshoot; Geneva/Schaller et al.: moderate overshoot; Becker: no overshoot. Error bars indicate $1\sigma$; mass is in $M_\odot$; luminosity is in $L_\odot$.

previous determination since it is dominated by the uncertainty in the velocity of the hot star, which is not bright enough to have been observed in the highest GHRS resolution. The mass is essentially the same as that found by Gorynya et al. (1995) and Evans & Sugars (1997) and the constraints on the evolutionary tracks in Figure 5 are little changed from the previous solutions.

We can use these masses to estimate the inclination plane of the orbit and the line of sight (54°) and deproject the semimajor axis of the Cepheid to 1.65 AU.

The questions arise whether reasonably the high eccentricity (0.37) would result in any tidal interaction, which might affect the evolution of the system or the period. For a typical radius of a five-day Cepheid ($\simeq$50 $R_\odot$), tidal forces even at periastron would only be $\simeq$1%. The rate of period change (Section 3 above) is not unusual for a star of this period, and hence likely to be dominated by evolution through the instability strip. In an earlier phase the Cepheid had a larger radius as a red giant. Strong constraints on interactions at this stage come from the discussion of the Z Lac binary system (Sugars & Evans 1996). Z Lac has the shortest orbital period for a Milky Way Cepheid (383 days). It is also the only binary Cepheid with an eccentricity indistinguishable from 0.0. The implication is that the orbit was circularized during the red giant phase, but that other Cepheids with wider separations retained the orbital eccentricity. V350 Sgr has a much longer orbital period than Z Lac, and retains its eccentricity, and hence is unlikely to have interacted even in the red giant stage.

For the LMC Cepheid in an eclipsing binary (Pietrzynski et al. 2010), however, this is an important question. It has a shorter orbital period (309 days) than any galactic binary Cepheid, and it seems likely that Roche lobe overflow has taken place in the red giant phase. This is particularly true since the two components are similar in evolutionary phase and both components were likely to be swollen to red giants at similar times.

The measured masses of Cepheids currently available are summarized in Figure 5. The mass of S Mus (Evans et al. 2006) was determined in the same way as V350 Sgr; however, the velocities of the companion were obtained from the highest resolution GHRS spectra. FF Aql and W Sgr come from *HST* Fine Guidance System (FGS) astrometry (Benedict et al. 2007; Evans et al. 2009). The Polaris astrometric system was resolved by *HST* (Evans et al. 2008). SU Cyg is based on IUE velocities (Evans & Bolton 1990). The luminosities have been calculated from the $M_V$ from the Leavitt Law (period–luminosity relation) from the *HST* FGS parallaxes of Benedict et al. (2007). Colors (corrected for the companions) have been taken from Evans (1995). The first overtone period of Polaris has been converted to a fundamental using the prescription of Alcock et al. (1995). Bolometric corrections are from Flower (1996) as discussed in Torres (2010). The scatter in the FGS parallaxes corresponds to an uncertainty about the size of the large symbols in Figure 5. For comparison, luminosities from the blue loop tips are plotted for several values of convective overshoot (no overshoot: Becker 1981; mild overshoot: Schaller et al. 1992 and Bertelli et al. 1994; full overshoot: Bertelli et al. 1986).

The first point Figure 5 illustrates is that in the last few years, several new techniques have been used to determine masses (e.g., Polaris, W Sgr, and FF Aql). In the future, improved data, for example, for Polaris and V350 Sgr, may reduce the error bars significantly.

The two issues most likely to affect the comparison of the measured masses with theoretical calculations are main-sequence convective overshoot and mass loss. For the current measured masses, all except SU Cyg indicate a moderate amount of overshoot and only for Polaris is the measured value as large as predicted by extreme overshoot. Overshoot or rotation, of course, may vary from star to star. Questions such as whether

there is a variation in these parameters which affect the size of the He core can be addressed in the future if the accuracy of the masses can be improved.

The question of mass loss has received new input in recent observational (Marengo et al. 2010) and theoretical (Neilson et al. 2011) studies. Again, future investigations will indicate whether the infrared emission in the field of $\delta$ Cep (Marengo et al.) is produced by mass loss and also whether it is prevalent in other Cepheids.

In summary, we have used extensive new data covering 10 orbital cycles (with particular improvement to the orbital velocity amplitude) to derive a new binary orbit for the classical Cepheid V350 Sgr. The new orbit is used to update the Cepheid mass measured for the star of $5.0 \pm 0.8\ M_{\odot}$.

It is a pleasure to acknowledge comments from Frank Fekel on the draft of this paper. We also thank the referee for constructive comments leading to an improved version. N.R.E. acknowledges support from the *Chandra* X-ray Center NASA Contract NAS8-03060. The present study was supported by research funding awarded through the Russian Foundation of Basic Research (grant 10-02-00489) to L.N.B. N.G. is grateful to Dr. P. Moskalik (Copernicus Astronomical Centre, Warsaw, Poland) for his advice, helpful discussions, and permanent support of radial velocity measurements. Her work was also partly supported by KBN grants 2-P03D-011-14, 5-P03D-011-30 and MNiSV grant 1-P03D-011-30 (Poland). A.R. and N.G. are grateful to Russian Foundation for Basic Research (grants 05-02-16526, 08-02-00738) for permanent support of observations.

## REFERENCES

Albitzky, V. 1930, Astron. Nachr., 238, 9
Alcock, C., Allsman, R. A., Axelrod, T. S., et al. 1995, AJ, 109, 1653
Arellano Ferro, A., Rojo Arellano, E., Gonzales-Bedolla, S., & Rozenzweig, P. 1998, A&AS, 117, 167
Barnes, T. G., Moffett, T. J., & Slovak, M. H. 1988, ApJS, 66, 43
Becker, S. A. 1981, ApJS, 45, 475
Benedict, G. F., McArthur, B. E., Feast, M. W., et al. 2007, AJ, 133, 1810
Berdnikov, L. N. 1992, Sov. Astron. Lett., 18, 207
Berdnikov, L. N., & Caldwell, J. A. R. 2001, J. Astron. Data, 7, 3
Berdnikov, L. N., Ignatova, V. V., & Vozyakova, O. V. 1997, A&AT, 14, 237
Berdnikov, L. N., Ignatova, V. V., & Vozyakova, O. V. 1998, Astron. Astrophys. Trans., 17, 87
Berdnikov, L. N., & Turner, D. G. 1995, Astron. Lett., 21, 717
Berdnikov, L. N., & Turner, D. G. 1998, Astron. Astrophys. Trans., 16, 291
Berdnikov, L. N., & Turner, D. G. 2000, Astron. Astrophys. Trans., 18, 679
Berdnikov, L. N., & Turner, D. G. 2001, Astron. Astrophys. Trans., 19, 689
Berdnikov, L. N., & Turner, D. G. 2004, Astron. Astrophys. Trans., 23, 253
Berdnikov, L. N., & Turner, D. G. 2006, Astron. Astrophys. Trans., 25, 327
Berdnikov, L. N., & Vozyakova, O. V. 1995, Astron. Lett., 21, 308
Bertelli, G., Bressan, A., Chiosi, C., & Angerer, K. 1986, A&AS, 66, 191
Bertelli, G., Bressan, A., Chiosi, C., Fagatto, F., & Nasi, E. 1994, A&AS, 106, 275
Bono, G., Caputo, F., & Castellani, V. 2006, Mem. Soc. Astron. Ital., 77, 207
Bruntt, H., Evans, N. R., Stello, D., et al. 2008, ApJ, 683, 433
Caldwell, J. A. R., Coulson, I. M., Dean, J. F., & Berdnikov, L. N. 2001, J. Astron. Data, 7, 4
Caputo, F., Bono, G., Fiorentino, G., Marconi, M., & Musella, I. 2005, ApJ, 629, 1021
Cassisi, S., & Salaris, M. 2011, ApJ, 728, L43
Dean, J. F. 1977, Mon. Notes Astron. Soc. South. Afr., 36, 3
Eaton, J. A., & Williamson, M. H. 2007, PASP, 119, 886
Eggen, O. J. 1951, ApJ, 113, 367
Eggen, O. J. 1985, AJ, 90, 1297
ESA. 1997, The *Hipparcos* and *Tycho* Catalogues (ESA SP-1200; Noordwijk: ESA)
Evans, N. R. 1995, ApJ, 445, 393
Evans, N. R., & Bolton, C. T. 1990, ApJ, 356, 630
Evans, N. R., Böhm-Vitense, E., Carpenter, K., Beck-Winchatz, B., & Robinson, R. 1997, PASP, 109, 789
Evans, N. R., Massa, D., Fullerton, A., Sonneborn, G., & Iping, R. 2006, ApJ, 647, 1387
Evans, N. R., Massa, D., & Proffitt, C. 2009, AJ, 137, 3700
Evans, N. R., Schaefer, G. H., Bond, H. E., et al. 2008, AJ, 136, 1137
Evans, N. R., & Sugars, B. J. A. 1997, AJ, 113, 792
Feltz, K. A., & McNamara, D. H. 1980, PASP, 92, 609
Filin, A. Ya. 1950, Tsirc. Stalinabad Astron. Obs., N77-78, 3
Florya, N. F., & Kukarkina, N. P. 1953, TrSht, 23, 3
Flower, P. J. 1996, ApJ, 469, 355
Gieren, W. 1981a, ApJS, 46, 287
Gieren, W. 1981b, ApJS, 47, 315
Gorynya, N. A., Irsmambetova, T. R., Rastorgouev, A. S., & Samus, N. N. 1992, Sov. Astron. Lett., 18, 316
Gorynya, N. A., Samus, N. N., Berdnikov, L. N., Rastorgouev, A. S., & Sachkov, M. E. 1995, Inf. Bull. Var. Stars, 4199, 1
Gorynya, N. A., Samus', N. N., Rastorguev, A. S., & Sachkov, M. E. 1996, Astron. Lett, 22, 175
Gorynya, N. A., Samus', N. N., Sachkov, M. E., et al. 1998, Astron. Lett., 24, 815
Hertzsprung, E. 1919, Astron. Nachr., 210, 17
Irwin, J. B. 1961, ApJS, 6, 253
Joy, A. H. 1937, ApJ, 86, 363
Keller, S. C. 2008, ApJ, 677, 483
Kukarkin, B. V. 1940, TrSht., 13, 118
Lloyd Evans, T. 1980, SAAO Circ., 1, 257
Marengo, M., Evans, N. R., Barmby, P., et al. 2010, ApJ, 725, 2392
Mitchell, R. I., Iriarte, B., Steinmetz, D., & Johnson, H. L. 1964, Bol. Obs. Tonantzintla Tacubaya, 3, 153
Moffett, T. J., & Barnes, T. G. 1984, ApJS, 55, 389
Neilson, H. R., Cantiello, M., & Langer, N. 2011, A&A, 529, L9
Parenago, P. 1930, Astron. Nachr., 238, 11
Parenago, P. P. 1938, TrSht, 12, 1
Petterson, O. K. L., Cottrell, P. L., & Albrow, M. D. 2004, MNRAS, 350, 95
Pietrzynski, G., Thompson, I. B., Gieren, W., et al. 2010, Nature, 468, 542
Pojmanski, G. 2002, Acta Astron., 52, 397
Schaller, G., Schaerer, D., Meynet, G., & Maeder, A. 1992, A&AS, 96, 269
Stobie, R. S. 1970, MNRAS, 148, 1
Sugars, B. J. A., & Evans, N. R. 1996, AJ, 112, 1670
Tokovinin, A. A. 1987, Sov. Astron., 31, 98
Torres, G. 2010, AJ, 140, 1158
Voute, J. 1932, Annalen Bosscha Sterrenwacht, 2, D37
Walraven, Th., Mueller, A. B., & Oosterhoff, P.Th. 1958, Bull. Astron. Inst. Neth., 14, 81